ISBN: 978-3-95450-247-9 ISSN: 2673-5490 doi: 10.18429/JACoW-IPAC2024-MOPR42

PREPARATION FOR REALISATION OF EXTERNAL ELECTRON INJECTION FOR AWAKE RUN 2B

N. Z. van Gils,*[1] M. Turner, V. Bencini,[3] E. Gschwendtner, G. Zevi Della Porta[2]
CERN, Geneva, CH
F. Pannell, University College London, London, UK
L. Ranc, Max Planck Institute for Physics, Munich, DE
A. Gerbershagen, PARTREC, UMCG, University of Groningen, Groningen, NL
[1] also at PARTREC, UMCG, University of Groningen, Groningen, NL
[2] also at Max Planck Institute for Physics, Munich, DE
[3] also at John Adams Institute for Accelerator Science, University of Oxford, Oxford, UK

Abstract

The Advanced Wakefield Experiment (AWAKE) aims to accelerate electrons to particle physics relevant energies using self-modulated proton bunches as drivers in a single plasma. AWAKE is now in its Run 2b (2023-2024), where the goal is to stabilise wakefields by using a plasma density step. Experimental demonstrations require probing of the longitudinal wakefields by externally injected electron bunches. To optimise charge capture in the wakefields, the electron beam density should be maximised at the site of injection z_e. This is achieved by setting the beam waist at z_e. Since no diagnostics are currently available at these locations, waist beam sizes are extrapolated from measurements upstream. The qualitative and quantitative agreement obtained between measured and simulated transverse electron beam sizes, at locations where these can be measured, demonstrates good understanding of the beam line optics and provides confidence in the extrapolated beam sizes at waist locations, where these cannot be measured. This information can then be used in the experiment to maximise the beam density at the site of injection.

THE AWAKE EXPERIMENT

AWAKE is an R&D experiment at CERN with the aim to develop proton-driven based plasma wakefield acceleration. The wakefields are driven by highly-relativistic (400 GeV, relativistic factor $\gamma_{p+} \sim 427$) and energetic (> 19 kJ) proton bunches, supplied by the CERN Super Proton Synchrotron (SPS). Since these proton bunches are longer than the plasma wavelength λ_{pe} (where $\lambda_{pe} = 2\pi c/\omega_{pe}$, with $\omega_{pe} = \sqrt{n_{pe}e^2/\epsilon_0 m_e}$ is the plasma electron frequency, c the speed of light, m_e the electron mass, e the electron charge, ϵ_0 the vacuum permittivity and n_{pe} the plasma electron density) and less dense than the plasma ($n_b <\sim 10^{-3} n_{pe}$, where n_b is the bunch density), the proton bunches have to be self-modulated to excite wakefields with GV/m amplitudes [1, 2]; this requires $n_{pe} > 10^{14}$ cm^{-3} (corresponding to $\lambda_{pe} < 3$ mm). The plasma is created by laser ionisation (pulse length: ~100 fs, energy per pulse: ~100 mJ, central wavelength: 800 nm) of rubidium vapour [3, 4]. It is 10 m long, with a radius >~1 mm. Seeded proton bunch self-modulation and subsequent wakefield growth, as well as the acceleration of externally injected witness electrons was demonstrated in AWAKE Run 1 [5–7].

Numerical simulation studies show that the use of a plasma density step (during the development of self-modulation) allows for stabilisation of the field amplitudes after saturation of self-modulation [8, 9]. The purpose of the ongoing experimental campaign (Run 2b [8]) is to demonstrate the effectiveness of a density step. One method to achieve this goal consists in measuring increased energy gain of accelerated witness particles. AWAKE requires external injection as wakefields are of relatively low amplitude (~0.5 GV/m) and high phase velocity (relativistic factor $\gamma \sim \gamma_{p^+} \sim 427$) [10, 11]. Furthermore, the witness electron bunch must be injected off-axis and several meters into the vapour source at a location z_e, (typical $z_e \sim 2$−4 m), avoiding loss of witness particles to wakefield phase shifts occurring at the beginning of self-modulation or during a density step [8].

For Run 2b, a new vapour source was developed and installed [12]. Due to its complexity, there is currently no beam diagnostic inside of it. The transverse beam size and shape at injection can thus only be predicted using optics simulations, as detailed in [13].

In this article, the presented agreement of measured and simulated beam sizes at the entrance of the vapour source for different optical setups (beam waist between $z_e = 2$ and 9 m) confirms good understanding of the beam evolution in simulations. In previous work, [13], an estimate of the maximum injection angle as a function of z_e was presented, and required these beam parameters as input.

THE ELECTRON BEAM LINE

A schematic drawing of the electron beam line is shown in Fig. 1. The electrons are produced by illuminating a Cs_2Te cathode with a UV laser pulse (typical spot size: ~1 mm, average energy: 200 nJ, top hat intensity profile) [14, 15]. Changing the illuminated surface area of the cathode allows varying of the electron bunch charge between 100−800 pC, as measured at a Faraday cup (see Fig. 1). First, electrons are

* nikita.zena.van.gils@cern.ch

ISBN: 978-3-95450-247-9 ISSN: 2673-5490 doi: 10.18429/JACoW-IPAC2024-MOPR42

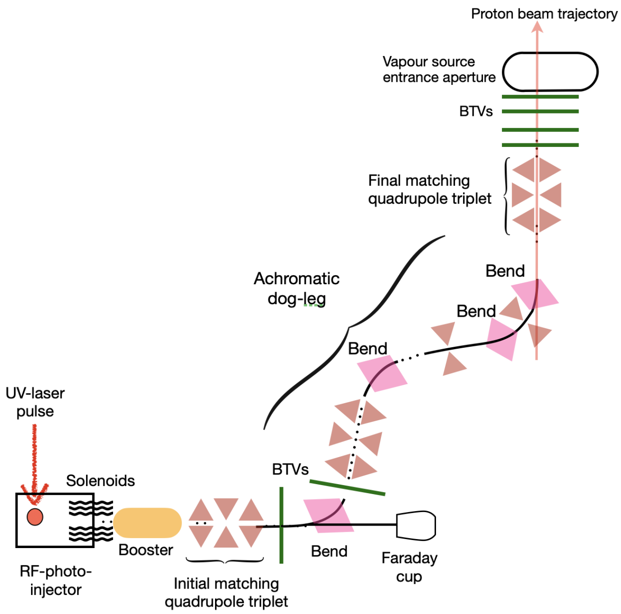

Figure 1: Schematic drawing of the electron gun and the 15m long beam transport line. Beam propagates to the right and up on the page. Bends are horizontal and vertical.

accelerated to ~5 MeV and bunched in an S-band RF-photo-injector [16] while simultaneously focused by two solenoids. Next, electrons are further accelerated to ~19 MeV by a 1 m-long travelling wave booster structure [17, 18]. A 15 m long transfer line transports the ~19 MeV electrons towards the vapour source. Two kicker magnets located 3.2 and 1 m upstream the vapour source entrance allow to realise the off-axis injection scheme detailed in [13].

The electron beam transfer line can be split into: 1) a matching section (quadrupole triplet), to couple the bunch produced by the RF photo-injector gun into the beam line; 2) an achromatic dogleg, to align the electron beam onto the proton beam trajectory, transporting the beam within facility constraints; and 3) a quadrupole triplet that allows to focus the electron beam at the desired location z_e. In total, the transfer line comprises eleven quadrupoles, four dipoles (two horizontal and two vertical), twelve corrector magnets (both horizontal and vertical), and eleven beam position monitors (BPMs) [19].

The transverse beam distribution and centroid position can be monitored along the transfer line on one of six scintillating YAG screens (BTVs), located 13.27, 12.15, 2.72, 1.25, 0.71 and 0.09 m upstream the vapour source entrance, shown in Fig. 1. The last two BTVs upstream of the vapour source entrance are used to set the injection geometry. The ~19 MeV electron bunches experience significant scattering (on the order of ~20 to 100 mrad) when traversing a beam screen. Measurements can therefore only be performed at one screen at a time.

OPTICAL SETUP

For injection experiments, the electron bunch is set to cross the wakefields at a given longitudinal location z_e inside of the vapour source, where $z_e = 0$ m is defined to be at the entrance aperture. To maximise charge captured into the wakefields, the transverse beam size should be minimal at z_e, and comparable to or smaller than the radial extent of the wakefields, which is in the order of a plasma skin depth c/ω_{pe}; ranging from $c/\omega_{pe} \sim 100$ to ~600 µm for plasma electron densities used in AWAKE. Since the beam size can currently not be measured at z_e, agreement between the measured and simulated beam distributions along the transfer line must be used to extrapolate these sizes.

Optimisation Of Beam Line Optics

It was found operationally that optimisation of the beam transport optics (to achieve a target beam size at the desired location) using analytical matching and linear optics is accurate if beams (produced by the photo-injector) are well represented by Gaussian distributions and if the initial conditions of the electron beam are close to the design specifications [20].

Frequently, however, produced beams are not necessarily Gaussian and crucial information, such as cross-plane correlations in the initial beam distribution or the exact central momentum, may even be unknown. In that case, it was found that more advanced methods improve operational optics tuning. Typically, the algorithm optimises as follows: the beam Twiss parameters are measured (either with quadrupole scan or tomographic reconstruction) at the entrance of the beam line and are used as input for tracking simulations. The optimal strengths of the initial (used to match the electron beam out of the gun to the beam line) and final (used to move the waist to z_e) triplet (see Fig. 1) are then found using a numerical optimiser that matches the beam parameters at injection to the nominal ones [21]. With these, transport of the electron beam and a minimal transverse size for each z_e is achieved.

The beam line also comprises dispersive components (bends) and their dispersion is compensated via dedicated quadrupoles along the line, see Fig. 1. However, after matching the beam to the beamline, the field strengths of the magnets in these section remains mostly unchanged.

BEAM SIZES AT THE ENTRANCE APERTURE AND BEAM

On Fig. 2 (top), the measured horizontal ($2\sigma_x$: black) and vertical ($2\sigma_y$: red) transverse electron beam sizes 9 cm upstream of the vapour source entrance for beam waist positions inside the vapour source $z_e = 2$ to 9 m, in steps of 1 m, are displayed. Beam sizes are extrapolated from Gaussian fits to the projected transverse distributions (further discussion on the beam size analysis can be found in [13]). Measurements were performed with an electron bunch charge of ~275 pC, (measured at the Faraday Cup shown on Fig. 1) and an initial normalised emittance of 1.03 ± 0.14 and 1.63 ± 0.51 mm mrad in x and y, obtained via quadrupole scan using the second quadrupole in the initial matching triplet. Measured beam sizes were obtained by Gaussian fits of the

ISBN: 978-3-95450-247-9 ISSN: 2673-5490 doi: 10.18429/JACoW-IPAC2024-MOPR42

2D beam distributions imaged on YAG screens. Error bars include position jitters and uncertainties of fit results.

Additionally shown, on Fig. 2 (top), are the simulated beam sizes, that were obtained in two ways: 1) by Gaussian fits to the transverse beam profiles obtained from tracking the beam distribution reconstructed with tomography [21] (dashed lines on Fig. 2) and 2) tracking the optics functions ($\beta_{x,y}$, $D_{x,y}$) to the screen location (dotted lines on Fig. 2) with $\sigma_{x,y} = \sqrt{\epsilon\beta_{x,y} + (D_{x,y}\delta p/p)^2}$, where $\delta p/p \sim 5\%$. Both tracking methods use the MADX [22] code. The second method is less computationally expensive, but does not take additional parasitic effects (known misalignment of certain magnetic elements) into account, resulting in less accurate predictions.

Measurements on Fig. 2 show that, as expected, $\sigma_{x,y}$ increases with larger z_e. Additionally, these measurements are performed very close to the entrance aperture and therefore allow to define the maximum combination of z_e and injection angle without significant injection losses, using Eq. 1 in [13]. As detailed in [13], if electrons interact with the entrance aperture, they are lost, reducing the amount of charge entering the vapour source. For example for $z_e = 2$ and 4 m, under certain assumptions, an estimated maximum injection angle without significant losses is 2.5 and 1.25 mrad.

The very good agreement between measurements and simulations shown on Fig. 2 enables electron beam size estimates at z_e (where there are no diagnostics) from simulations. Simulation results show that beam sizes range between 200 and 300 µm from $z_e = 2$ to 9 m, and are therefore within the desired order of c/ω_{pe}. Note that larger sizes would not only reduce the beam charge density at the site of injection, but also increase the injection location uncertainty [13].

Because of electron beam losses at the entrance and exit apertures, the charge transmitted through the vapour source is less than 100 %. Transmission measurements can therefore be used to test beam size predictions by comparing them to calculations based on theoretical beam sizes. Figure 2 (bottom) shows the calculated (green) and measured (black) charge transmitted, as a fraction of the input charge, through the vapour source for different focal points.

The input charge was measured using the Faraday cup at the beginning of the electron beam line, see Fig. 1. The transmitted charge was measured at a beam-current-transformer located 6 m downstream of the vapour source exit. Error bars include jitters on the measurements on both the upstream Faraday cup and downstream beam current transformer. As expected, between $z_e = 2$ to 6 m, the charge transmission increases as the beam size at the exit aperture (not shown) decreases. For $z_e > 6$ m, transmission decreases as losses occur at the entrance aperture (see blue horizontal bands on Fig. 2). Note that measurements are non-symmetric with z_e because of the different geometry of the entrance (racetrack shape sizes 8 mm horizontal and 3 mm vertical) and exit apertures (round with $r = 5$ mm). While qualitative agreement is excellent, the consistent 10–20 % quantitative offsets are under investigation.

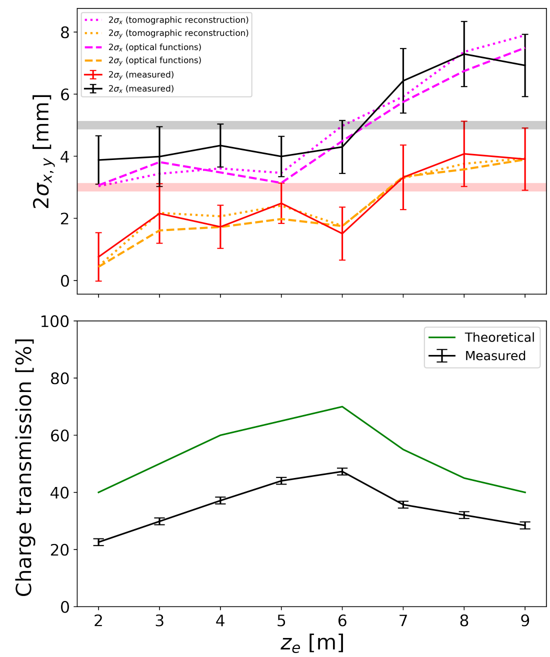

Figure 2: Top: 2σ beam sizes measured on the last upstream screen prior to the entrance aperture as a function of the focal point (and therefore beam waist) position inside the vapour source. Red and black lines show the result of experimental measurements. Orange and purple dotted (dashed) lines show the resulting beam size from tracking optical functions (tomographic reconstruction). Horizontal bands indicate vapour source entrance and exit limitations (upstream in red 3 mm and downstream 5 mm in grey). Bottom: Fraction of charge measured on transmitted through the vapour source (black) and theoretical considerations (green) for different focal points.

Figure 2 only shows results for $z_e \geq 2$ m. Injecting (and therefore focusing) at $z_e < 2$ m would be non-ideal due to wakefield phase shifts (either occurring during the development of self modulation or by means of a density step) or defocusing effects in the plasma entrance ramp, and measurements are therefore not included in Fig. 2.

CONCLUSION

Electron beam size studies required for the realisation of the AWAKE Run 2b electron injection experiments are summarised. Firstly, electron beam sizes measured close to the vapour source entrance are shown and can provide input to calculate the maximum injection angle for a given focal point location [13]. Secondly, qualitative and quantitative agreement between simulated and measured transverse beam sizes upstream the vapour source entrance allows to confirm that electron beam sizes (from simulations) at the wakefield crossing points are in the order of the plasma skin depth, and therefore acceptable for injection experiments. Finally, qualitative agreement between the observed and estimated trend of charge transmission further confirms agreement between simulations and measurements.

ISBN: 978-3-95450-247-9 ISSN: 2673-5490 doi: 10.18429/JACoW-IPAC2024-MOPR42

REFERENCES

[1] C. B. Schroeder, C. Benedetti, E. Esarey, F. J. Grüner, and W. P. Leemans, "Growth and phase velocity of self-modulated beam-driven plasma waves", *Phys. Rev. Lett.*, vol. 107, p. 145002, 2011. `doi:10.1103/PhysRevLett.107.145002`

[2] N. Kumar, A. Pukhov, and K. V. Lotov, "Self-modulation instability of a long proton bunch in plasmas", *Phys. Rev. Lett.*, vol. 104, p. 255003, 2010. `doi:10.1103/PhysRevLett.104.255003`

[3] G. Demeter *et al.*, "Generation of 10-m-lengthscale plasma columns by resonant and off-resonant laser pulses", *Optics and Laser Technology*, vol. 168, p.109921, 2024. `doi:10.1016/j.optlastec.2023.109921`

[4] V. Fedosseev *et al.*, "Integration of a terawatt laser at the CERN SPS beam for the AWAKE experiment on proton-driven plasma wake acceleration", in *Proc. 7th Int. Particle Accelerator Conf. (IPAC'16)*, Busan, Korea, May 2016, paper WEPMY020, pp. 2592-5. `doi:10.18429/JACoW-IPAC2016-WEPMY020`

[5] K. V. Lotov *et al.*, "Natural noise and external wakefield seeding in a proton-driven plasma accelerator", *Phys. Rev. ST Acc. Beams*, vol. 16, p. 041301, April 2013. `doi:10.1103/PhysRevSTAB.16.041301`

[6] F. Batsch, *et al.* (AWAKE Collaboration), "Transition between instability and seeded self-modulation of a relativistic particle bunch in plasma", *Phys. Rev. Lett.*, vol. 126, p. 164802, 2021. `doi:10.1103/PhysRevLett.126.164802`

[7] E. Adli *et al.* (AWAKE Collaboration), "Acceleration of electrons in the plasma wakefield of a proton bunch", *Nature*, vol. 561, pp. 363-7, 2018. `doi:10.1038/s41586-018-0485-4`

[8] E. Gschwendtner *et al.* (AWAKE Collaboration), "The AWAKE run 2 programme and beyond", *Symmetry* vol. 14, p. 1680, 2022. `doi:10.3390/sym14081680`

[9] K. V. Lotov, "Physics of beam self-modulation in plasma wakefield accelerators", *Phys. Plasmas*, vol. 22 p. 103110, 2015. `doi:10.1063/1.4933129`

[10] C. B. Schroeder *et al.*, "Growth and phase velocity of self-modulated beam-driven plasma waves", *Phys. Rev. Lett.*, vol. 107, p. 145002, 2011. `doi:10.1103/PhysRevLett.107.145002`

[11] K. V. Lotov *et al.*, "Electron trapping and acceleration by the plasma wakefield of a self-modulating proton beam", *Phys. Plasmas*, vol. 21, p. 123116, 2014. `doi:10.1063/1.4904365`

[12] P. Muggli *et al.*, "Plasma light as diagnostic for wakefields driven by developing self-modulation of a long particle bunch", in *Proc. 20th Adv. Acc. Concepts Workshop (AAC'22)*, Long Island, NY, USA, 2022.

[13] N. Z. van Gils *et al.*, submitted to *Proc. 6th European Advanced Accelerator Concepts Workshop (EAAC'23)*, 2023.

[14] V. Fedosseev *et al.*, "Generation and delivery of an ultraviolet laser beam for the RF-Photoinjector of the AWAKE electron beam", in *Proc. 10th Int. Particle Accelerator Conf. (IPAC'19)*, Melbourne, Australia, May 2019, paper THPGW054, pp. 3709-12. `doi:10.18429/JACoW-IPAC2019-THPGW054`

[15] M. Martinez-Calderon *et al.*, "Fabrication and rejuvenation of high quantum efficiency caesium telluride photocathodes for high brightness and high average current photoinjectors", *Phys. Rev. Accel. Beams*, vol. 27, p. 023401, 2024. `doi:10.1103/PhysRevAccelBeams.27.023401`

[16] Y. Kim *et al.*, "Commissioning of the electron injector for the AWAKE experiment", *Nucl. Instrum. Meth. in Phy. Res.* A, vol. 953, p.163194, 2020. `doi:10.1016/j.nima.2019.163194`

[17] K. Pepitone *et al.*, "The electron accelerators for the AWAKE experiment at CERN baseline and future developments", *Nucl. Instrum. Meth. in Phy. Res.* A, vol. 909, pp 102-6, 2018. `doi:10.1016/j.nima.2018.02.044`

[18] J.S. Schmidt *et al.*, "Status of the proton and electron transfer lines for the AWAKE Experiment at CERN", *Nucl. Instrum. Meth. in Phy. Res.* A, vol. 829, pp 58-62, 2016. `doi:10.1016/j.nima.2016.01.026`

[19] S. Mazzoni *et al.*, "Beam instrumentation developments for the advanced proton driven plasma wakefield acceleration experiment at CERN", in *8th Proc. Int. Particle Accelerator Conf. (IPAC'17)*, Copenhagen, Denmark, May 2017, paper MOPAB119, pp. 404-7. `doi:10.18429/JACoW-IPAC2017-MOPAB119`

[20] C. Bracco *et al.*, "Systematic optics studies for the commissioning of the AWAKE electron beamline", in *10th Proc. Int. Particle Accelerator Conf. (IPAC'19)*, Melbourne, Australia, May 2019, paper WEPMP029, pp. 2383-6. `doi:10.18429/JACoW-IPAC2019-WEPMP029`

[21] V. Bencini *et al.*, "Beam characterization and optimisation for AWAKE 18 MeV electron line", in *14th Proc. Int. Particle Accelerator Conf. (IPAC'23)*, Venice, Italy, 2023, paper MOPA103, pp. 291-4. `doi:10.18429/JACoW-IPAC2023-MOPA103`

[22] MAD-X PTC, Multi-particle tracking `http://mad.web.cern.ch/mad/`